Geomechanics and Engineering, *Vol. 27, No. 6 (2021) 561-571*
https://doi.org/10.12989/gae.2021.27.6.561

Effects of new construction technology on performance of ultralong steel sheet pile cofferdams under tidal action

Ping Li[a], Xinfei Sun, Junjun Chen and Jiangwei Shi*

Key Laboratory of Ministry of Education for Geomechanics and Embankment Engineering, Hohai University, Nanjing, Jiangsu 210024, China

(Received July 31, 2021, Revised October 19, 2021, Accepted November 18, 2021)

Abstract. Cofferdams made of teel sheet piles are commonly utilized as support structures for excavation of sea-crossing bridge foundations. As cofferdams are often subject to tide variation, it is imperative to consider potential effects of tide on stability and serviceability of sheet piles, particularly, ultralong steel sheet piles (USSPs). In this study, a real USSP cofferdam constructed using new construction technology in Nanxi River was reported. The design of key parts of USSP cofferdam in the presence of tidal action was first introduced followed by the description of entire construction technology and associated monitoring results. Subsequently, a three-dimensional finite-element model corresponding to all construction steps was established to back-analyze measured deflection of USSPs. Finally, a series of parametric studies was carried out to investigate effects of tide level, soil parameters, support stiffness and construction sequence on lateral deflection of USSPs. Monitoring results indicate that the maximum deflection during construction occurred near the riverbed. In addition, measured stress of USSPs showed that stability of USSP cofferdam strengthened as construction stages proceeded. Moreover, the numerical back-analysis demonstrated that the USSP cofferdam fulfilled the safety requirements for construction under tidal action. The maximum deflection of USSPs subject to high tide was only 13.57 mm at a depth of -4 m. Sensitivity analyses results showed that the design of USSP cofferdam system must be further improved for construction in cohesionless soils. Furthermore, the 5th strut level before concreting played an indispensable role in controlling lateral deflection of USSPs. It was also observed that pumping out water before concreting base slab could greatly simplify and benefit construction program. On the other hand, the simplification in construction procedures could induce seepage inside the cofferdam, which additionally increased the deflection of USSPs by 10 mm on average.

Keywords: construction design; deflection monitoring; three-dimensional finite-element analysis; tidal action; ultralong steel sheet pile cofferdam

1. Introduction

It is conventional to utilize cofferdams as temporary support for excavation of sea-crossing bridge foundations. There are many kinds of support types for cofferdams, e.g., cellular and double-walled sheet pile. Of all different supporting systems, cofferdams made of thin-walled steel structures are commonly used to retain hydrostatic and hydrodynamic pressure due to its cost-effectiveness and convenience for installation (Qu *et al*. 2016, Shi *et al*. 2018, Wang *et al*. 2017, Singh *et al*. 2020).

Several studies have been devoted to investigating working performance of thin-walled structure cofferdams. For example, Arboleda-Monsalve *et al*. (2018) found that the lateral deformation of the cofferdam increased fourfold if gaps existed between sheet piles and steel ring beams during construction. It was also observed that cofferdams for sea-crossing bridges could get damaged or even collapse if subject to extreme wave loads during tropical cyclones (e.g., Xu, *et al*. 2015a, Xu, *et al*. 2015b, Kang *et al*. 2020). Ti *et al*. (2018) conducted field monitoring and numerical back-analysis of a real cofferdam during typhoon Dujuan in 2015 and found that tide-induced pressure spectral characteristics of cofferdams were different from that under normal flow conditions. In addition, Gui *et al*. (2009) reported a failed cofferdam, which was caused by the dislocation of the weld joints. Follow-up numerical back-analyses revealed the it was important to choose an appropriate support system with adequate safety margin and flexibility to account for the inherent variability of sheet pile installation.

Apart from structural integrity, hydraulic failure is also a key factor governing stability of a cofferdam. Benmebarek *et al*. (2005) adopted finite difference method to analyze the seepage failure of sandy soil within a cofferdam and found that friction angle and dilatant behaviors of sandy soil played a key role in controlling hydraulic failure. Tanaka *et al*. (2013) carried out experimental and numerical analyses to investigate 3D seepage failure of a cofferdam in sand. It was observed that the larger the enclosed area of a cofferdam was, the greater the three-dimensionally concentrated seepage flow was. Other researchers (e.g., Noh *et al*. 2012, Ozcelik 2016, Wang *et al*. 2019) focused on axisymmetric modelling of 3D seepage failure and investigated effects of plan shape of a cofferdam on theoretical critical hydraulic gradient.

Previous studies reveal that the stability of cofferdam

*Corresponding author, Ph.D. Associate Professor
E-mail: ceshijiangwei@163.com

ISSN: 2005-307X (Print), 2092-6219 (Online)

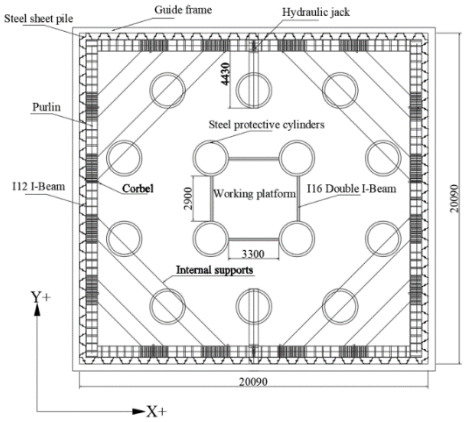

(a) Layout plan of USSPs cofferdam

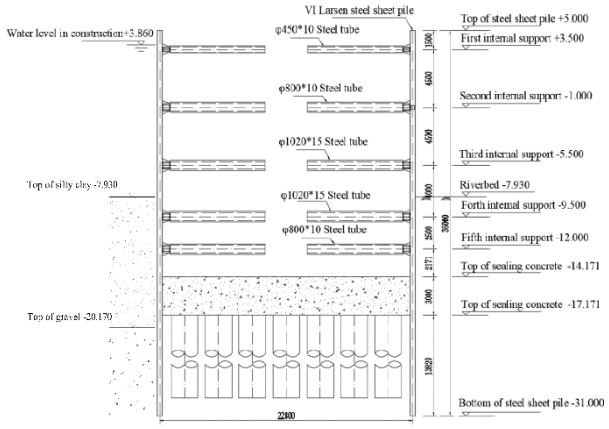

(b) Cross-section of USSP cofferdam structure

(c) Overview of constructed USSP cofferdam

Fig. 1 Geometry of USSP cofferdam structure

can be significantly affected by installation/construction of sheet piles and hydraulic seepage. More importantly, USSPs can easily break into deep-seated soils while maintaining the flexibility to adapt to foundations of different shapes. Despite of above-mentioned advantages, the application of USSPs still faces many challenges, which require further investigation.

(1) The variable underwater environment poses great uncertainties to design and construction of cofferdam structures, particularly, buoyancy control and crack resistance control (Fall *et al*. 2019, Li *et al*. 2020). The precise control of positioning, insertion and gap control of USSPs under tidal action requires innovative construction technology.

(2) Conventional sheet pile wall construction mainly focuses on estimation of internal stress after pumping or at final installation stage of support structures (Lefas and Georgiannou 2001, Jiang *et al*. 2018). A precise control of USSP deformation requires identification of key intermediate construction procedures, which initiate adverse USSP deformation, particularly, under tidal action.

(3) USSP cofferdam is large in scale and more prone to suffer complex loading conditions, such as hydrostatic pressure, hydrodynamic pressure, earth pressure (Zhao *et al*. 2018) and seepage impact (Lee *et al*. 2005). It is required to obtain an optimal engineering performance of USSP cofferdam even under adverse seepage impact, unfavorable soil parameters and construction conditions.

This study aims to solve the above three challenges via a real case study. The design of USSPs cofferdam system with an explicit consideration of buoyancy control and crack resistance control was introduced first followed by description of key construction technology of USSPs cofferdam. Subsequently, a numerical back-analysis was carried out to identify key parameters governing the deformation of USSPs under tidal action. Finally, a series of numerical parametric studies were conducted to investigate sensitivity of USSPs subject to different tide levels, seepage impact forces, soil parameters and construction conditions.

2. Nanxi river bridge project

2.1 Site condition

In this study, the cofferdam is part of the piers for Nanxi River Bridge project, which is located at the downstream of the Nanxi River. Since the location of this project is far from the sea, the Nanxi River water and groundwater river have no acid erosion. The mean annual water level of Nanxi River during the construction works was +3.86 m. Based on measurements from nearby observation station, Nanxi River has two high tides every day with a time interval of 12 hours between high tide and low tide. The water level difference between the high and low water levels can be up to 6 meters.

The subsurface geology is mainly composed of silty clay and round gravel soil. The silty clay has a high compressibility and sensitivity. The elevation of riverbed is -7.93 m, corresponding to a total water depth of 11.79 m.

2.2 Geometry of cofferdam structures

Fig. 1 shows the geometry and cross-section of the bridge pier cofferdam. The *X* and *Y* in Fig. 1(a) denote directions in parallel and in perpendicular to water flow direction, respectively. The cofferdam is rectangular in plan with a length (*a*) and a width (*b*) of 20.9 m and 20.9 m, respectively. In total, 14 steel drums with a radius, *R*, of 1.15 m were installed to support the bridge pier. A temporary working platform with an elevation, *H*, of -17.17 m was supported by the central four steel drums, which were connected using I16 double I-Beam. In this study, the length of steel sheet pile is 36 m, which is twice that of conventional sheet pile. The ultralong steel sheet pile walls can be installed quickly and recycled after construction. Thus, the cost is relatively low compared with other construction technique, such as reinforced concrete wall. The ultralong steel sheet pile walls have much better waterproof than cellular and double-walled sheet piles. The cross-section of cofferdam is shown in Fig. 1(b). The final excavation level was -17.171 m, corresponding to 9.241 m below the riverbed. Five strut levels plus a 3 m concrete basement were designed to stabilize the cofferdam. Fig. 1(c) shows the constructed USSP cofferdam.

2.3 Stability control of cofferdam

Due to a large plan area of the cofferdam, there was a high risk of seepage failure. A sealing concrete basement with adequate thickness and strength should be designed for USSP to resist potential buoyancy and crack resistance.

2.3.1 Determination of concrete thickness

Let the design thickness of the concrete cover be h_d. The net plan area of the sealing concrete is $S = a \times b - 14 \times \pi R^2$ after removing the area occupied by 14 steel drums. Corresponding hydrostatic water pressure (*P*) imposed on the upper surface of sealing concrete can be estimated using the following Eq.:

$$P = \gamma_w \times (H + h_d) \times S \tag{1}$$

where γ_w is unit weight of water and taken as 9.8 kN/m^3.

The gravitational pressure of the sealing concrete is calculated using Eq. (2),

$$G = \gamma_c \times S \times h_d \tag{2}$$

where γ_c is unit weight of concrete and taken as 24 kN/m^3.

According to 'Code for design of building foundation', the design bonding pressure between concrete and steel sheathing is 120 kPa. Using this value, associated bonding force, Q_1, between sealing concrete and steel drums can be estimated.

$$Q_1 = 14 \times 2\pi R \times 120 \times h_d \tag{3}$$

Similarly, the bonding force Q_2 between sealing concrete and steel sheet piles is calculated as follows.

$$Q_2 = 2 \times (a + b) \times 120 \times h_d \tag{4}$$

The uplift stability is guaranteed if $\frac{G+Q_1+Q_2}{P} > f_s = 1.05$. The resulted minimum value of h_d is 2.6 m. Considering potential floating slurry and entrapped mud on the top and bottom surfaces of sealing concrete, the design thickness of the sealing concrete h_d is determined to be 3.0 m.

2.3.2 Determination of concrete strength

After pouring sealing concrete and pumping out trapped water inside cofferdam, large water pressure can be imposed on the bottom of sealing concrete. The generated bending force within an unreinforced concrete slab can possibly cause concrete crack, posing a threat to the safety of USSP system. The net water pressure, *P*, acting on the bottom surface of sealing concrete can be calculated as the difference between hydrostatic water pressure and self-weight of concrete slab.

It is widely acknowledged that quality of concrete cured underwater is worse than that of ordinary concrete. As the slab is designed to concrete directly with in-situ pile foundations. It is reasonable to simplify base slab as a bidirectional slab with a four-point simple support. When a uniformly distributed net water pressure load is applied, the mid-span bending moments M_x and M_y can be calculated using Eq. (5).

$$M_x = \alpha_x \times P \times l_x^2, \qquad M_y = \alpha_y \times P \times l_y^2 \tag{5}$$

where α_x and α_y are the bending moment coefficients in perpendicular directions; *P* is net water pressure; l_x and l_y are the minimum calculation spans in corresponding directions. According to the 'Code for design of a building foundation' l_x and l_y are taken as 5.2m and 5.6m. Following the recommendation of the code, α_x and α_y are set as 0.0923 and 0.1113, respectively. The net water pressure can be calculated as $P = \gamma_w \times (H + h_d) - \gamma_c \times h_d$. Substituting *P* and h_d calculated from section 2.3.1 into above Eq. (5), corresponding bending moments M_x and M_y are equal to 345.19 kN·m and 416.25 kN·m, respectively.

Bending induced maximum tensile stress within the concrete slab can be estimated as $\sigma = \frac{1.2M_y}{W}$, where $W = b \times h_d^2/6$. The resulted maximum tensile stress within concrete slab is $\sigma = \frac{1.2M_y}{W} = 0.48\ MPa$, which is far smaller than the design tensile strength of 1.27 MPa for C25 concrete.

2.4 Key construction procedures

Construction technology plays a key role in determining the working performance of USSP system. In the following, several innovative construction technologies are summarized.

(1) As shown in Fig. 2(a), a guide frame was first installed to ensure that the driving positions of sheet piles were not affected by adverse tidal action. Subsequently, corbels were welded on the steel tube followed by assembling outer guide frame. The dual guide frames served as a strengthening ring to prevent the deviation of driving sheet piles.

(2) Lift the first steel sheet pile and place it along the guide frame under a gentle tide condition (see Fig. 2 (b)).

(a) Install the guide frame

(b) Insert steel sheet piles

(c) Lift and place enclosing purlin

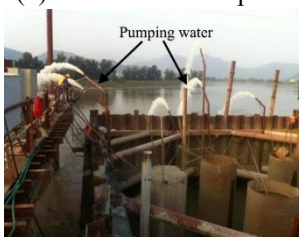

(d) Pump water out of cofferdam

(e) Groove welding

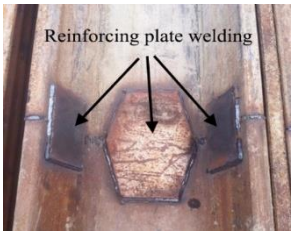

(f) Weld reinforcing plate

Fig. 2 Key construction technologies

The driving position was precisely controlled using a displacement-limiting device, and the verticality was constantly monitored and adjusted. After installing the first sheet pile, subsequent piles were inserted symmetrically and successively on both directions of cofferdam with the interlocking of previously installed pieces.

(3) During the construction process, USSPs inevitably inclined outwards the cofferdam by approximately 10 mm, which could affect the closure of cofferdam. Therefore, an offset was reserved for the first pile along each site of cofferdam. Another measure to eliminate potential inclination is to insert the last five groups of piles simultaneously into the dual guide frames, followed by successive driving.

(4) The steel protective cylinders for 10 circumferential steel drums in Fig. 1(a) were cut off so as to make room for the internal support system. A temporary operation platform for installing the enclosing purlin system was set up with a steel sheet pile and the central four protective steel cylinders (see Fig. 2(c)). The position of the enclosing purlin was adjusted continuously with the assistance of six rotation oil tops and the enclosing purlin is installed at -1m, -5.5 m, -9.5 m and -12 m. Subsequently, a qualified diver measured the gap between the enclosing purlin and USSPs. A steel pad was installed to ensure a tight contact between steel sheet piles and the enclosing purlin.

(5) After reaching the excavation depth of -14.171 m and putting up all five layers of struts, water and mud inside cofferdam were sucked away with an air compressor (see Fig. 2(d)).

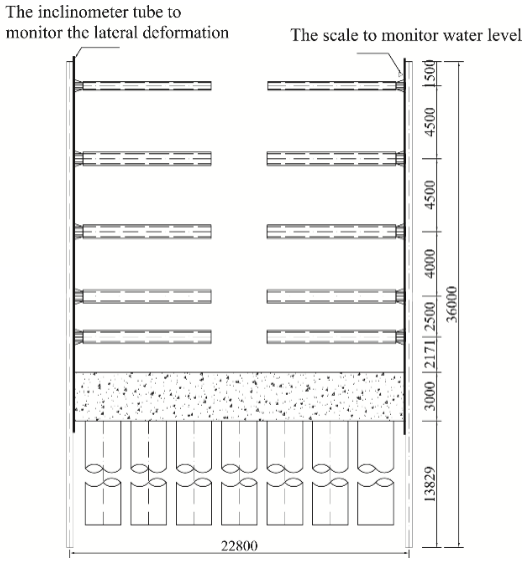

Fig. 3 Instrumentation and monitoring setup

To ensure the quality of subsequent sealing concrete slab, a diver was employed to clean the base surface and remove slimes that were stuck to the steel plate pile wall and the protective steel cylinders until reaching the excavation depth of -17.171 m. A bailey beam was set up to measure the base elevation at every 50cm during the sucking process, which was to ensure that the thickness of base sediment was no more than 10cm.

(6) Short USSPs were welded together using groove welding, and each joint was further strengthened using six reinforcing plates, which were symmetrically distributed on both sides of a joint (see Figs. 2(e) and 2(f)). The length of each reinforcing plate was 50cm and associated width was determined according to the actual size of the welding position. The thickness of each plate should not be less than that of the piles. Any two piles welded together should be aligned in line and any deviation was corrected by a heat gun.

2.5 Instrumentation

Due to a large tide variation, large deformation and internal forces can be induced in USSPs. For example, during high tide, there is a large water level difference inside and outside cofferdam, creating a large pressure difference.

In this project, steel sheet pile wall is constructed for cofferdam for sea-crossing piers. Obviously, the safety of the entire construction process is affected by lateral deformation of sheet pile wall. If excessive lateral deformations are induced, the entire structure may collapse and threaten the constructor. Although the sheet pile wall is a temporary structure, the lateral deformation should be monitored. Fig. 3 shows the instrumentation and monitoring setup. Two inclinometers for lateral deformation monitoring were installed in the middle of two perpendicular cofferdam walls to measure lateral deformation along different directions. In addition, two measuring points were set inside and outside the cofferdam to monitor water level.

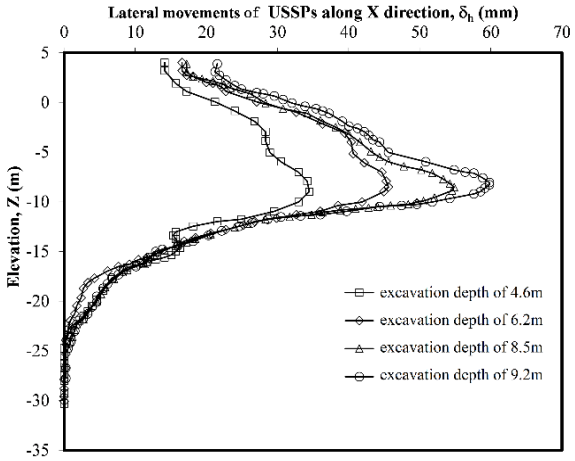

(a) Lateral deformation of the USSP along X direction

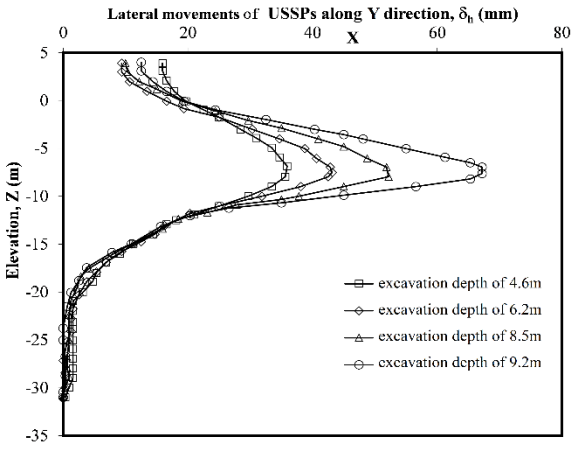

(b) Lateral deformation of the USSP along Y direction

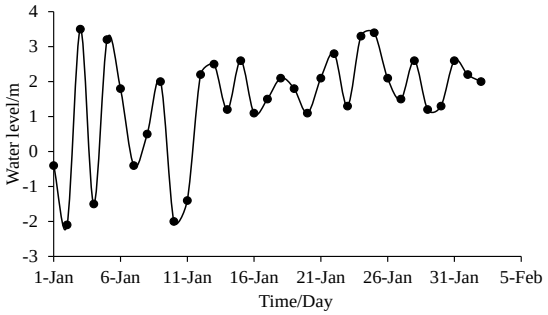

(c) Water level

Fig. 4 Measured lateral deformation of USSPs

2.6 Monitoring results

Fig. 4(a) shows measured lateral deflection of sheet pile walls with depth at different excavation depths. A positive deflection value denotes movement inward cofferdam. Note that lateral deflection was measured under high tide, which represented the worst construction scenario. As shown in Fig. 4(a), the maximum increases in the lateral wall movements occur when the excavation depth is varied from 4.6 m to 6.2 m. This is because the fifth struth is installed at the excavation depth of 4.6 m. When excavation depth varies from 4.6 m to 6.2 m, there is no any installation of struct. The lateral deflection along *X* direction increased when the depth was above -12.5 m and gradually reduced to 0 when depth further increased. This can be explained by the fact that the rigid bottom sealing platform was poured at -12.5 m. As construction proceeded, the lateral deflection increased. A maximum lateral deflection of about 60 mm was observed at a depth of -12.5 m, at the excavation depth of 9.2 m. The maximum lateral deflection ranged from +35 mm and +60 mm during excavation. A smaller lateral deflection of about +26 mm occurred at top of sheet pile wall due to the constraint of guide frames. Similarly, a maximum lateral deflection of +68 mm along *Y* direction was developed at a depth of -12.5 m at the excavation depth of 9.2 m (see Fig. 4(b)).

Fig. 4(c) shows the time plot of measured axial stress. For better comparison, the variation of water level was also superimposed. The water level periodically varied between -2.3 m and +3.7 m between 1Jan and 12 Jan. Before 6 Jan, the variation in water level is relatively fast. When the tide rises and falls, water pressure acting on the outer surface of sheet pile wall is changed. The elevations of high and low tide are +3.7 and -2.3 m, respectively. After 12 Jan, the fluctuation of water level reduced to between +1.0 m and +2.0 m. The results show in Fig. 4 underscores the importance of taking tide effects into design and construction of USSPs.

3. Three-dimensional Finite-Element Analysis

Based merely on the measured deflection and stress obtained from field monitoring, it was not possible to deduce the deformation mechanism of USSP cofferdam under tidal action. To assist in identifying key factors governing performance of USSP cofferdam, three-dimensional finite-element analysis was carried out to simulate the construction process of USSP cofferdam. More specifically, ABAQUS was adopted to investigate deformation mechanism of USSP cofferdam.

3.1 Model setup

Fig. 5 shows the established three-dimensional finite-element mesh used to back-analyse the field results described before. Due to symmetry of USSP cofferdam, only ¼ field scale was modelled to reduce computational

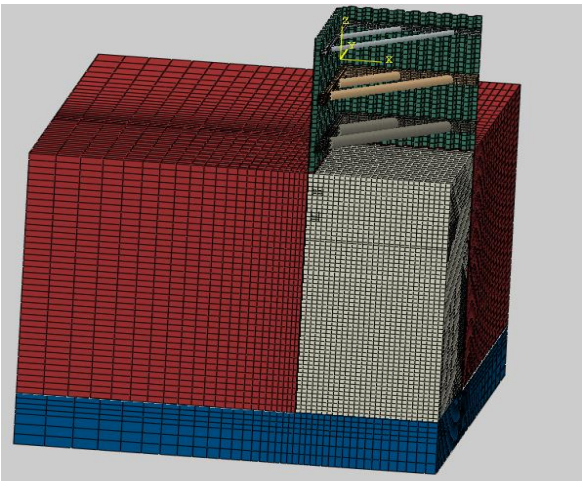

Fig. 5 Three-dimensional finite-element mesh

cost. This three-dimensional mesh had a length of 32 m, and a width of 32 m. The final excavation depth (H_e) of this basement was 9.24 m. Obviously, the distance between the sheet pile wall and the mesh boundary was 2.22 times of the final excavation. As reported by several studies (Hsieh and Ou 1998, Shi *et al*. 2020, Shi *et al*. 2022), the major influence zone of ground movement due to basement excavation was 2 H_e. Thus, effects of boundary conditions on the computed results are negligible. The total depth (Z) of the model was 28 m. Movements and rotations in all directions were fixed at the bottom of the model. Roller boundaries were adopted for all four external vertical boundaries.

In Fig. 5, red and blue colors represent silty clay and gravel, respectively. The elevations of water table and soil stratum were added in the Fig. 1(b). In this site, the elevations of water table and river bed were at +3.860 m and -7.930 m, respectively. Moreover, the elevations of silty clay and gravel were at -7.93 m and -20.17 m, respectively. In other words, the thickness of silty clay was 12.24 m.

In the analysis, the subsoil was modelled by solid element C3D8R. I-beam was simulated by shell elements S4R (no stress concentration) and S4 (stress concentration). The B31 element was used to simulate beam element, which supported struts. To ensure accuracy and improve efficiency of calculation, a tie constraint was adopted between the soil mass and the USSPs. In total, the three-dimensional finite element model comprised 120,077 elements, including 5,600 steel sheet pile elements, 106,746 soil elements and 7,731 internal support elements. By conducting a numerical parametric study, effects of mesh density on computed results were investigated. By increasing the number of current mesh by 100%, the difference of the maximum wall deflation was less than 2%. It is indicated that the current 3D mesh was fine enough.

In the numerical analysis, effects of tidal action on the performance of ultralong steel sheet pile are simulated by applying equivalent water pressure along the outer surface of sheet pile wall. The maximum change of water level due to tidal action is 6 m (i.e., elevations of high and low tidal levels are +3.7 and -2.3 m, respectively). After establishing the initial geostatic stress, the equivalent cyclic water pressure of 60 kPa is applied to the ultralong sheet pile wall. In each calculation step, this equivalent water pressure is circulated 20 times to simu Table 1. Summary of soil properties adopted for the finite element analysis

late the tidal action in cofferdam construction.

Table 1 Summary of soil properties adopted for the finite element analysis

Soil layer	γ (kN/m^3)	C (kPa)	φ' (deg)	Φ (deg)	E (MPa)	v
Silt soil	16.1	6.96	16	0.1	12	0.30
Round gravel soil	19.6	2.00	28	5.0	80	0.25

Note: γ = unit weight; E = Young's modulus; v = Poisson's ratio; c = effective cohesion; φ' = effective friction angle; Φ= dilatancy angle

Table 2 Summary of material properties for structural elements

Materials	E (MPa)	P (kg/m^3)	v
C25 Concrete	2.8×10^4	2400	0.25
Steel sheet pile	2.1×10^5	7800	0.30
Internal support	2.1×10^5	7800	0.30

3.2 Model parameters

Soil behaviors were simulated using an elastoplastic model with a Mohr-Coulomb failure criterion. The M-C model can capture key features of soil behaviors and model parameters can be easily determined. But the M-C model cannot capture soil stiffness varied from stress and strain levels. This study focuses on the lateral deformations of ultralong steel sheet pile wall rather than soil movements due to basement excavation. The lateral wall deformations of sheet pile wall are controlled by pressure balance, and soil movements are dominated by soil stiffness. If soil pressures applying on the sheet pile wall are accurately simulated, the lateral wall deformations of sheet pile wall can be reasonably predicted regardless of soil models.

Table 1 summarizes material properties adopted for the finite-element analysis. The soil unit weight (γ) is measured by cutting ring method, and the cohesion and frictional angle of soils are measured by direct shear test.

All structural elements were modelled as linear elastic behavior. Table 2 summaries physical and mechanical properties of concrete, steel sheet pile and struts.

According to 'General Specification for Design of Highway Bridge and Culvert (JTG D60-2015)', the characteristic value of hydrodynamic pressure f_w acting on a bridge pier can be estimated as follows.

$$f_w = K \times \frac{\gamma V^2}{2g} \tag{6}$$

where γ is unit weight of water; V is water flow velocity; A is the cross-sectional area of a bridge pier subject to hydrodynamic pressure; g is the gravitational acceleration; and K is the shape factor and takes as 1.5 for a square cofferdam. Following Eq. (6), the hydrodynamic pressure f_w

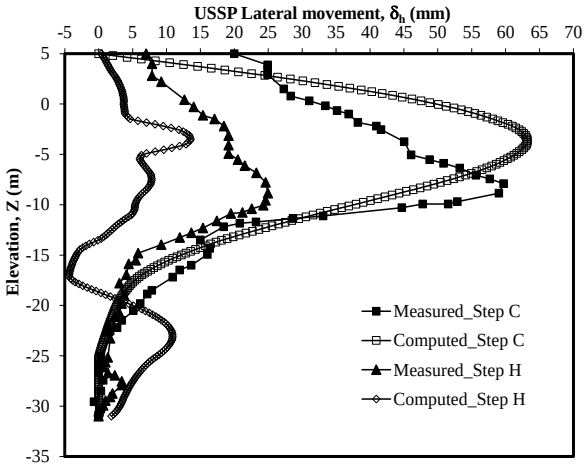

Fig. 6 Comparison of USSP deflection

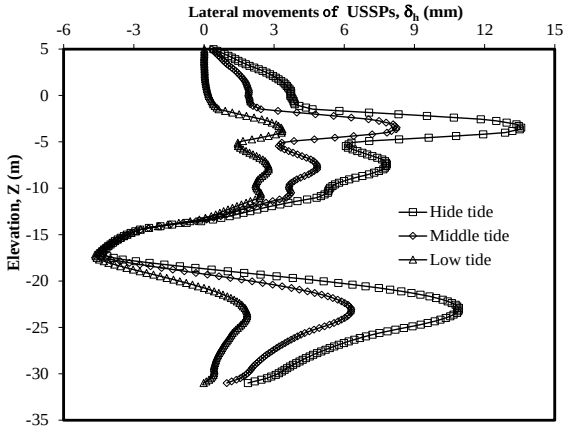

Fig. 7 Deflection of USSPs under different tide levels

acting on USSPs was computed to be 9.162 kPa.

3.3 Numerical modelling procedures

The construction sequence was simplified and modelled as follows.

(a) Establish geostatic stress state and import into the original model to simulate in-situ soil stress state.

(b) Install USSPs one by one and activate associated hydrostatic and flow pressures on installed USSPs.

(c) Suction water and mud inside cofferdam to 0.5 m below the 1st strut level followed by installation of beams and struts.

(d) Repeat step (c) until all five levels of struts were installed and excavation reached 0.5 m below the final strut level.

(e) Dredge soil inside cofferdam to the final excavation level followed by laying a 50 cm thick graded gravel layer.

(f) Lay a 50 cm thick graded stone cushion to the designed bottom elevation of sealing concrete and activate the 2.8 m thick concrete. The process of concrete hardening was simulated by modifying stiffness and strength.

(g) Change the static water pressure inside the cofferdam, and simulate the process of water pumping from the cofferdam after the design strength of sealing concrete was reached.

(h) Remove the 5th strut level after pumping water inside the cofferdam followed by pouring 0.2 m thick sealing concrete.

3.4 Interpretation of computed results

Fig. 6 compares the computed and measured lateral deflection of USSP cofferdam during mud absorption (step c) and concrete pouring (step h). The measured deflection during mud suction stage had a maximum value of 60 mm. The magnitude was close to the computed value of 65 mm. The top level of pile exhibited a deflection of about 18 m. Because of disturbance caused by construction machines surrounding the site, non-zero deflection is observed at the top of sheet pile wall. In comparison, the computed deflection was 0mm at pile top due to rigid constraint from guide frame during simulation process. In addition, computed and measured deflection curves for concrete pouring at step g were also plotted for comparison. Both computed and measured deflection values decreased substantially to less than 25 mm.

4. Parametric study of USSP-soil interaction

The good agreement between measured and computed deflections as discussed in previous section validates the finite element model. In this section, a series of parametric studies was carried out to investigate effects of tide levels, soil parameters, support system stiffness and construction sequences on deflection of USSPs.

4.1 Effects of different tide levels on USSP deflection

As the USSP cofferdam reported in this study was located in deep water and subject to a large tide variation. The level difference between high and low tide can be up to 6m. Therefore, it is imperative to analyze the stress and deformation performance of USSP cofferdam structures under different tide conditions. Static and hydrodynamic pressures acting on cofferdam wall were simulated to increase linearly with depth. The elevations of high, middle and low tide levels are +3.7, +0.7 and -2.3 m, respectively. Obviously, the changes in water table due to tidal action is as high as 6 m. Since the elevation of river bed is -7.93 m, the corresponding water depths are 11.63, 8.63, and 5.63 m, respectively.

Fig. 7 shows computed lateral deflection of USSPs at the final construction stage (i.e., step H). Essentially, the lateral deflection curve increased when tide level rose. The computed deflection at pile top was equal to 0 mm due to the perfect constraint from displacement limiting device. At low tide, the deflection varied between -5 mm (outwards movement) and +3 mm (inwards movement). The maximum positive deflection of 3.07 mm occurred at a depth of -4 m (between 2nd and 3rd struct level) and increased to 8.22 mm and 13.57 mm at middle and high tides, respectively. The deflection reduced gradually with depth and reached zero at the elevation (i.e., -17 m) of

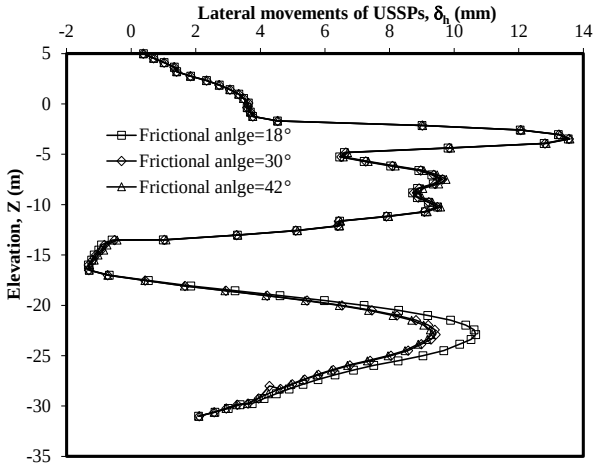

Fig. 8 Deflection of USSPs subject to different soil friction angles

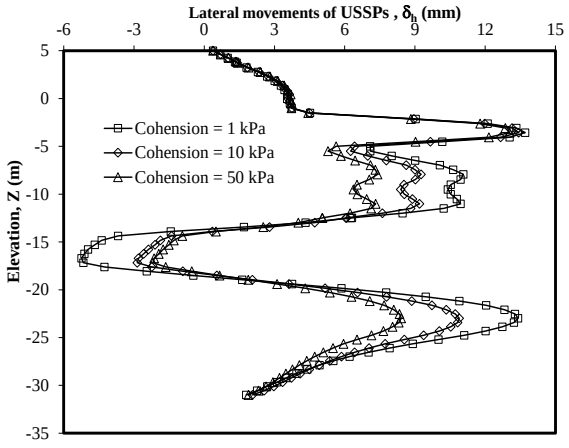

Fig. 9 Deflection of USSPs subject to different soil cohesions

sealing concrete layer. It is noted that tide induced deflection can be up to 10mm, which should be taken into consideration during serviceability and stability analysis of USSPs system. For this project, irrespective of tide level, the maximum lateral deflection of USSPs was less than the allowable value of 14 mm.

4.2 Effects of soil parameters on USSP deflection

In the numerical analysis, parameters of soils within and outside the cofferdam are changed. In the numerical parametric study, effects of frictional angle and cohesion of soil are explored. The soil frictional angles are 18°, 30° and 42°, corresponding to silty clay, sandy silt and coarse sand, respectively (Zhou 2020, Wang 2015, Liu *et al*. 2021). Moreover, the cohesions of soil are designed as 1, 10 and 50 kPa, corresponding to silt, silty clay and hard-plastic red clay (Li *et al*. 2020, Wang 2015, Cao *et al*. 2020).

Fig. 8 shows computed deflections at the final construction stage (i.e., step H) using different soil friction angles. The maximum deflection of about 13.89 mm occurred at a depth of -4.0 m. A subpeak deflection of -10.67 mm below final excavation level (i.e., -17.17 m) was developed at a depth of about -22 m when the friction angle was 18°. The subpeak value reduced to 9.43 mm and 9.29 mm when the internal friction angle increased to 30° and 42°, respectively.

In this construction site, the water depth is 11.79 m. The lateral wall deformation at the upper part of sheet pile wall is controlled by water pressure, regardless of soil frictional angle. The lateral movement of the USSP below -15 m increases as a decrease in soil frictional angle. As soil frictional angle varied from 42° to 18°, the maximum lateral wall deformation induced at the lower part of sheet pile wall is increased by 13%. As soil frictional angle is decreased, the coefficient of active Rankine earth pressure is increased, but the coefficient of passive Rankine earth pressure is decreased. Thus, a smaller soil frictional angle causes larger difference of pressures acting on sheet pile wall, resulting in larger lateral wall deformation. The results indicate that the increase in friction angle has a positive effect on constraining the lateral deflection of USSP cofferdam. More importantly, the relationship between the increase in friction angle and the decrease in deflection was non-linear, which implies that soil constraints imposed on USSP cofferdam gradually weakened as the soil shear strength increased.

Similarly, different cohesion values can also significantly affect lateral earth pressure. Fig. 9 shows computed deflection with depth using different cohesion values. The maximum deflection of about 13.5 mm occurred at a depth of approximately -4 m irrespective of adopted cohesion values. There was a great variation in deflection below riverbed (at -7.93 m) when different cohesion values were assigned. A maximum deflection of 8.41 mm was observed at a depth of approximately -23 m when soil cohesion was equal to 50 kPa. The deflection increased to 10.89 mm and 13.41 m when soil cohesion reduced to 10 kPa and 1 kPa, respectively. It is observed that USSP had a larger deflection in cohesionless soils, e.g., sandy soils, than in cohesive soils, e.g., clays. Therefore, it is recommended to collect multiple qualified samples from a target site to obtain an accurate estimation of cohesion before designing USSP system. It is also worth mentioning that soil cohesion has a greater influence on deflection of USSPs than soil friction angle.

4.3 Effects of support system stiffness on USSP deflection

Apart from geological and tide conditions, stiffness of support system can also affect lateral deflection of USSPs. In field, the fifth struct was removed after casting 3 m thick concrete slab. In numerical simulation, the fifth struct was not simulated for simplicity. In this section, the intermediate 5th strut level at a depth of -12 m in the original finite element model was removed in order to investigate effects of support stiffness on USSP deflection. It is anticipated that a reduction in stiffness of support system can lead to an enlarged lateral deflection.

Fig. 10 shows comparison of lateral deflection of USSPs at the final construction step (i.e., step H) with different levels of struts. Although the removed strut was at a depth

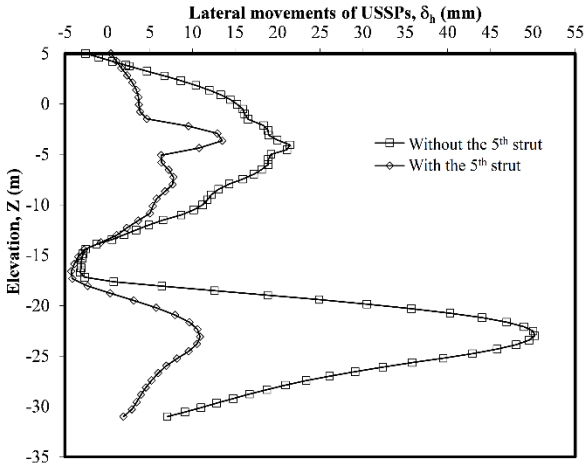

Fig. 10 Deflection of USSPs subject to different support stiffness

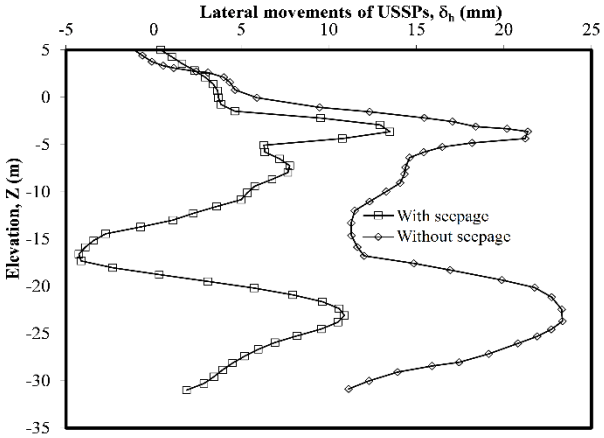

Fig. 11 Deformation of USSPs under seepage impact

of -12 m, the updated supporting system with four strut levels exhibited a maximum deflection of 50 mm at a depth of -23 m. The value was five times larger than the original model with five strut levels. It should be noted that the 5th strut level in the original model served as a platform for concreting works before dismantling. Therefore, the lateral deflection was greatly alleviated due to the additional constraint from the 5th strut level. Essentially, the variation in lateral deflection was a combined result of a change in tide water pressure, excavation and pumping within the cofferdam. Although the 5th struct level was finally removed after concreting base slab in Step H, it played an indispensable role in controlling deflection of the entire USSP cofferdam system.

4.4 Effects of construction sequence on USSP deflection

As sealing concrete was cured underwater, the engineering performance of USSP system was not subject to seepage effect (Yousefi *et al*. 2016, Madanayaka and Sivakugan 2019, Kamash *et al*. 2021). In this section, the construction sequence was switched to pump out water before constructing the concrete platform to investigate the influence of seepage. As a result of the new construction procedure, the 4th and 5th strut levels were not installed underwater, which greatly simplified construction works. On the other hand, seepage posed a new challenge for USSP system.

Fig. 11 compares the computed deflection with the explicit consideration of seepage effect. The maximum deflection occurred at the riverbed and the soft soil layer (at a depth of approximately -23 m). Deflection of USSPs calculated from the original model was negative at a depth of approximately -15 m, where the concrete platform was constructed. In comparison, when seepage effect was taken into consideration, deflection at this level became +12 mm. This was induced by pressure reduction inside cofferdam after water pumping. As plastic deformation within soils was already developed, the subsequent pouring of concrete platform could not eliminate seepage induced deflection.

Although the new construction sequence could benefit construction, an additional 10 mm deflection of USSPs on average could be induced. Note that the deflection of USSP cofferdam caused by the new construction sequence remained within the specified limit of 80 mm. In summary, the original construction sequence resulted in a smaller deflection of cofferdams, and the new sequence facilitated construction process and saved time.

5. Conclusions

In this study, field measurements from key construction procedures of USSP cofferdam were reported. A three-dimensional finite-element model was established to back-analyze the performance of USSP cofferdam. Subsequently, a series of parametric studies was carried out to investigate effects of tide level, soil parameters, support stiffness and construction sequence on lateral deflection of USSPs. Based on results of this study, the following conclusions may be drawn.

- The design and key construction technologies of USSP cofferdam under tidal action were introduced in detail. The monitoring data revealed that the measured stress and deflection of USSPs increased with an increase in tide level. The adverse effects induced by tidal action should be considered during design of USSP system.
- Excavation under high tide represented the worst construction scenario. Associated deflection curve indicated that the maximum deflection of 13.57 mm was observed at a depth of -4 m.
- Numerical sensitivity analysis found that soil cohesion could have a greater influence on deflection of USSPs than soil friction angle. USSP cofferdam might not be suitable for construction in sandy soils under tidal action.
- The 5th struct level provided a platform for concreting base slab and played an indispensable role in controlling deflection of USSP cofferdam.
- New construction sequence, which constructed base slab after water pumping operation, could greatly simplify construction procedures and significantly improve construction speed. However, the new construction sequence could induce seepage inside cofferdam, which on

average increased the deflection of USSP by approximately 10 mm. A balance should be sought between construction program and engineering performance of USSPs when selecting a construction scheme.

In this study, a relatively simple soil model (MC) is used to simulate soil behavior. Effects of soil stress and strain level on soil stiffness are not considered. It is suggested to adopt an advanced soil model to analyses soil movement and sheet pile wall deformation due to basement excavation.

Acknowledgments

The authors would like to acknowledge the financial support provided by the National Natural Science Foundation of China (Grant No. 41977240) and the Fundamental Research Funds for the Central Universities (No. B200202090).

References

Arboleda-Monsalve, L.G., Uribe-Henao, A.F. Velasquez-Perez, A , Zapata-Medina, DG and Sarabia, F. (2018), "Performance of urban cofferdams braced with segmental steel and reinforced concrete ring beams", *J. Geotech. Geoenviron. Eng.*, **144**(4), 04018015. https://doi.org/10.1061/(ASCE)GT.1943-5606.0001864.

Babu, G. and Basha, B.M. (2008), "Optimum design of cantilever sheet pile walls in sandy soils using inverse reliability approach", *Comput. Geotech.*, **35**(2), 134-143. https://doi.org/10.1016/j.compgeo.2007.04.001.

Benmebarek, N., Benmebarek S. and Kastner, R. (2005), "Numerical studies of seepage failure of sand within a cofferdam", *Comput. Geotech.*, **32**(4), 264-273. https://doi.org/10.1016/j.compgeo.2005.03.001.

Cao, W.T. and Gao, B. (2020), "Analysis of Guizhou original and Remolded Red Clay's shear strength indexes under different stress paths", *Heilongjiang Transport. Technol.*, **43**(09), 13-14. http://doi.org/10.16402/j.cnki.issn1008-3383.2020.09. 006.

Fall, M., Gao, Z. and Ndiaye, B.C. (2019), "Three-dimensional response of double anchored sheet pile walls subjected to excavation and construction sequence," *Heliyon*, **5**(3), e01348. https://doi.org/10.1016/j.heliyon.2019.e01348.

Gui, M.W. and Han, K.K. (2009), "An investigation on a failed double-wall cofferdam during construction", *Eng. Fail. Anal.*, **16**(1), 421-432. https://doi.org/10.1016/j.engfailanal.2008.06.004.

Hsieh, P.G., and Ou, C.Y (1998), "Shape of ground surface settlement profiles caused by excavation", *Canadian Geotech. J.*, **35**(6), 1004-1017. https://doi.org/10.1139/cgj-35-6-1004.

Jiang, S.Y., Du, C.B. and Sun, L.G. (2018), "Numerical analysis of sheet pile wall structure considering soil-structure interaction", *Geomech. Eng*, **16**(3), 309-320. https://doi.org/10.12989/gae.2018.16.3.309.

JTG D60 (2015), *General Specification for Design of Highway Bridge and Culvert*, Ministry of Transport of the People's Republic of China, Beijing, China.

Kang, A., Zhu, B., Lin, P., Ju, J. and Zhang, D. (2020), "Experimental and numerical study of wave-current interactions with a dumbbell-shaped bridge cofferdam", *Ocean Eng*, **210**, 107433. https://doi.org/10.1016/j.oceaneng.2020.107433.

Kamash, W.E., Naggar, H.E. and Nagaratnam, S. (2021), "Numerical analysis of lateral earth pressure coefficient in inclined mine stopes", *Geomech. Geophys. Geo.*, **7**(3), 61. https://doi.org/ 10.1007/s40948-021-00255-4.

Lee, J.Y., Choi, Y.K., Kim, H.S. and Yun, S.T. (2005), "Hydrologic characteristics of a large rockfill dam: implications for water leakage", *Eng. Geol.*, **80**(1-2), 43-59. https://doi.org/10.1016/j.enggeo.2005.03.002.

Lefas, I.D. and Georgiannou, V.N. (2001), "Analysis of a cofferdam support and design implications", *Comput. Struct.*, **79**(26-28), 2461-2469. https://doi.org/10.1016/S0045-7949(01)00082-7.

Li, D., Zhou, N.Q., Wu, X.N. and Yin, J.C. (2020), "Seepage-stress coupling response of cofferdam under storm surge attack in Yangtze estuary", *Mar. Georesour. Geotech.*, **39**(5), 515-526. https://doi.org/10.1080/1064119X.2020.1712630.

Li, X.X., Yang, Y.J., Zhao, Q. and Cui, J.W. (2020), "Influence of moisture content on mechanical parameters of soil", *J. Hunan City Univ.,* **29**(3), 16-19. https://doi.org/10.3969/j.issn.1672-304.2020.03.0004.

Liu, N. and Liu, J. (2021), "Comparison of methods for determining internal friction angle of sand by domestic and foreign standards", *Port Waterway Eng.*, **2021**(1), 42-47. http://doi.org/10.16233/j.cnki.issn1002-972.20201228.029.

Madanayaka, T.A. and Sivakugan, N. (2019), "Simple solutions for square and rectangular cofferdam seepage problems", *Can. Geotech. J.*, **56**(5), 730-745. https://doi.org/10.1139/cgj-2018-0295.

Noh, J., Lee, S., Kim, J.S. and Molinas, A. (2012), "Numerical modeling of flow and scouring around a cofferdam", *J. Hydro-Environ. Res.*, **6**(4), 299-309. https://doi.org/ 10.1016/j.jher.2011.08.005.

Ozcelik, M. (2016), "Assessment of engineering geological design parameters for Kandil (CFRD) Dam, Kahramanmaras-Turkey", *Bull. Eng. Geol. Environ.*, **75**(2), 1-11. https://doi.org/10.1007/s10064-015-0823-9.

Qu, H., Li, R., Hu, H., Jia, H. and Zhang, J. (2016), "An approach of seismic design for sheet pile retaining wall based on capacity spectrum method", *Geomech. Eng.*, **11**(2), 309-323. https://doi.org/10.12989/gae.2016.11.2.309.

Shi, J.W., Zhang, X., Chen, Y.H., Chen, L. (2018), "Numerical parametric study of countermeasures to alleviate basement excavation effects on an existing tunnel", *Tunn. Undergr. Sp. Tech.*, **72**, 145-153. https://10.1016/j.tust.2017.11.030.

Shi, J.W., Ding C., Ng, C.W.W., Lu, H. and Chen, L. (2020), "Effects of overconsolidation ratio on tunnel responses due to overlying basement excavation in clay", *Tunn. Undergr. Sp. Tech.*, **7**, 103247. https://doi.org/10.1016/j.tust.2019.103247.

Shi, J.W., Wei, J.Q., Ng, C.W.W., Lu, H., Ma, S.K., Shi, C., and Li P. (2022), "Effects of construction sequence of double basement excavations on an existing floating pile", *Tunn. Undergr. Space Technol.*, 119, 104230. https://doi.org/10.1016/j.tust.2021.104230.

Singh, A.P. and Chatterjee, K. (2020), "Lateral earth pressure and bending moment on sheet pile walls due to uniform surcharge", *Geomech. Eng.*, **23**(1), 71-83. https://doi.org/ 10.12989 /gae.2020.23.1.071.

Tanaka, T., Kusumi, S. and Inoue, K. (2013), "Effects of plane shapes of a cofferdam on 3D seepage failure stability and axisymmetric approximation", *In Proceedings of the 18th Int. Conf. Soil Mech. Geotech. Eng.*, 2103-2106. September.

Ti, Z., Wei, K., Qin, S., Mei, D. and Li, Y. (2018), "Assessment of random wave pressure on the construction cofferdam for sea-crossing bridges under tropical cyclone", *Ocean Eng*, **160**(15), 335-345. https://doi.org/ 10.1016/j.oceaneng.2018.04.036.

Wang, W.D., Li, Q., Hu, Y., Shi, J.W. and Ng, C.W.W. (2017), "Field investigation of collapse of a 13-story high-rise residential building in Shanghai", *J Perform. Constr. Fac*, **31**(4), 04017012. https://10.1061/(ASCE)CF.1943-5509.0001005.

Wang, J.F., Xiang, H.W. and Yan, J.G. (2019), "Numerical simulation of steel sheet pile support structures in foundation pit excavation," *Int. J. Geomech.*, **19**(4), 05019002.1-05019002.12. https://doi.org/ 10.1061/(ASCE)GM.1943-5622.0001373.

Wang, Z.J. (2015), Experimental Study of the Influence of Clay Content on Mechanical Properties of Unsaturated Soil", MPhil Dissertation, Zhejiang University of Technology, Hangzhou, China.

Xu, F., Li, S., Zhang, Q., Li, L., Zhang, Q., Wang, K. and Liu, H. (2015a), "Analysis and design implications on stability of cofferdam subjected to water wave action", *Mar Georesour. Geotech.*, **34**(2), 181-187. https://doi.org/10.1080/1064119X.2014.990125.

Xu, G., Cai, C. and Han Y. (2015b), "Investigating the characteristics of the solitary wave induced forces on coastal twin bridge decks", *J. Perform. Constr. Fac.*, 2016, **30**(4), 04015076. https://doi.org/10.1061/(ASCE)CF.1943-5509.0000821.

Yousefi, M., Sedghi-Asl, M. and Parvizi, M. (2016), "Seepage and boiling around a sheet pile under different experimental configuration", *J. Hydrol. Eng.*, **21**(12), 06016015. https://doi.org/ 10.1061/(ASCE)HE.1943-5584.0001449.

Zhao, T., Ding, W., Wei, L., Wu, W. and Qiao, Y. (2018), "The behavior analysis of a cofferdam constructed by double sheet pile wall above muck", *Proceedings of the Geoshanghai 2018 Int. Conf: Tunn. Underg. Construct*., Shanghai, China, May.

Zhou, Z.Y. (2020), *Research on the Parameters and Bearing Characteristics of Main Rock and Soil Layers in Xinyu City*", MPhil Dissertation, Nanchang University, Nanchang, China.

GC